EFDA–JET–CP(10)07/22

M. Vrancken, E. Lerche, T. Blackman, F. Durodié, M. Evrard, M. Graham,
P. Jacquet, A. Kaye, M.-L. Mayoral, M.P.S. Nightingale, J. Ongena,
D. Van Eester, M. Van Schoor and JET EFDA contributors

Performance of the Scattering Matrix Arc Detection System on the JET ITER-Like ICRF Antenna

Performance of the Scattering Matrix Arc Detection System on the JET ITER-Like ICRF Antenna

M. Vrancken[1], E. Lerche[1], T. Blackman[2], F. Durodié[1], M. Evrard[1], M. Graham[2], P. Jacquet[2], A. Kaye[2], M.-L. Mayoral[2], M.P.S. Nightingale[2], J. Ongena[1], D. Van Eester[1], M. Van Schoor[1] and JET EFDA contributors*

JET-EFDA, Culham Science Centre, OX14 3DB, Abingdon, UK

[1]Association EURATOM-Belgian State, Koninklijke Militaire School - Ecole Royale Militaire, B-1000 Brussels Belgium
[2]EURATOM-CCFE Fusion Association, Culham Science Centre, OX14 3DB, Abingdon, OXON, UK
** See annex of F. Romanelli et al, "Overview of JET Results", (Proc. 22nd IAEA Fusion Energy Conference, Geneva, Switzerland (2008)).*

Preprint of Paper to be submitted for publication in Proceedings of the 26th Symposium on Fusion Technology (SOFT), Porto, Portugal
27th September 2010 - 1st October 2010

ABSTRACT.
Ion Cyclotron Radio Frequency (ICRF) antennas operating under high voltage to couple high power to fusion plasmas are at risk of electrical arcing. The standard Voltage Standing Wave Ratio (VSWR) system does not protect low impedance areas, which are used in antennas to achieve load tolerance to variations in plasma loading during Edge Localised Modes (ELMs). The Scattering Matrix Arc Detection System (SMAD) was designed to create additional protection for these areas, and 4 complete systems were implemented and tested on the ITER-Like Antenna (ILA) on JET. This paper describes the performance under relevant experimental conditions of load tolerance and/or high voltage and electrical arcing causing generator trip events.

1. INTRODUCTION

The tolerance to load variations during ELMs of the ITER-Like Antenna (ILA) [1] is achieved by setting the impedance at the internal conjugate T-points to low impedance (~3Ω). When operated in this configuration, arcing occurring around the T-junctions is not detected by the standard Voltage Standing Wave Ratio (VSWR) protection [2]. Consequently, additional arc detection was developed to safely operate the ILA on ELMy H-mode. The SMAD system, technically completely described in [3] was fully implemented on the ILA and this paper describes its experimental performance during the JET experimental campaigns of 2008/2009. The analysis focuses on JET pulses with the ILA operating at high power and/or under load tolerant conditions and with generator trip events due to electrical arcing. The nature of the arc events (position, relation with ELMs,…) are investigated by analyzing the correlation between the VSWR, Sub-Harmonic Arc detection (SHAD [4]) and SMAD logical trip signals, high sampling rate RF data (from different measurements point along the system) and the computed SMAD error signals.

2. CONFIGURATION OF ILA ARC PROTECTION SYSTEMS

Figure 1 shows one quarter *E12* of the ILA (using JET antenna designation *E* and strap pair *kl=12*) with the standard $VSWR_{kl}$ protection system installed on the Main Transmission Line (MTL) close to the generator, and the SHAD [4] system reading the reflected voltage from the Antenna Pressurised Transmission Line (APTL) directional couplers. The $SMAD_{kl}$ system *kl=12,34,56,78* measures the probe voltages V_k,V_l and directional coupler signals V^+_{kl},V_{kl} to produce an error signal

$$SMAD_{kl} = \frac{K_{1kI}.V_k + K_{2kl}.V_I}{K^-_{kI} - K_{3kl}.V^+_{kI}} - 1 \qquad (1)$$

with 3 error coefficients $K_{ikl}(S_{3x3}(f),C_k,C_l,f)$ i=1,2,3 per strap pair *kl* determined from the RF model $S_{3x3}(f)$ matrix, measured capacitor positions C_k,C_l and operating frequency f [3]. The SMAD protected area on the ILA includes a section of the APTL with the VaCuum Window (VCW), the Vacuum Transmission Line (VTL) with the vacuum capacitors, but not the plasma facing antenna straps as indicated in Figure 1. The RF signals are converted by Analog to Digital Converters (ADC) to be used by the $SHAD_{kl}$, $VSWR_{kl}$ and $SMAD_{kl}$ arc detection electronics and also stored at different

sampling rates on the PXI real time matching computer (5*ms*), the SMAD PC (stored at 200μs and 2μs) and the general JET Pulse File (JPF) storage system (stored at 2.5*ms* and 5μs) [3]. All logical trip signals *kl=12,34,56,78* are also stored in the JPF and are all combined together in one big logical 'OR' operation to trip all 4 amplifiers simultaneously if one of the signals indicates a fault condition.

3. COMMISSIONING AND OPERATION OF THE SMAD

The SMAD system has been in development in parallel with the ILA antenna itself since the identification of the VSWR arc protection's ineffectiveness around the low-impedance T-point zone. Table 1 gives an overview of the final commissioning of the system on the JET-ILA, starting with the collection of experimental data by the SMAD hardware until the end of 2009 JET experiments. On each shot, the fast data acquisition on the SMAD system (2μs) alone records 500MB raw data, 150MB when compressed. The more relevant data is recorded in the last 160 RF pulses, where any outstanding technical problems [2] on the SMAD system had been resolved and the ILA antenna was operating in relevant load resilient and high voltage/power conditions.

In Figure 1, the settings of the SMAD system are computer controlled to be modified on a shot by shot basis. The trip level settings of the VSWR system and SHAD systems were adjusted manually for a series of pulses. Also, in practice, the SHAD logical output signal was not hardwired to trip the system but only monitored off-line. Finally, although the logical tripping signals were recorded, an investigation into the nature of the arcing events occurring over the 4 front interacting parts of the antenna requires human interpretation of the recorded data. At a first level, the PXI matching data and logical trip signals from the 3 arc protection systems allow to judge the operating conditions of the antenna and whether any tripping events occurred. At a second level, a reduced sampling rate (200μs) SMAD error signal indicates possible arc events. Finally, individual events are fully analysed through the fast RF and SMAD data, as illustrated by the examples in the next section.

4. ANALYSIS OF SELECTED TRIP EVENTS

Figure 2 (a) and (b) illustrate **JET Pulse No. 76231** with toroidal magnetic field $B_T = 2.7T$, plasma current $I_p = 2.0MA$ and plasma separatrix to first wall distance of 5.0*cm*. The Balmer α-line emission (traces 1) from recycled hydrogen clearly indicate the transition from L-to ELMy H-mode plasma with $P_{NBI} = 7.0MW$ Neutral Beam power Injection (NBI) at 14.0*s*. The ILA lower half E34+E78 is coupling a near constant $P_{ICRF} = 0.4MW$ at 42*MHz,* and the strap voltages (traces 2) increase from 18 to 24kV with the reduced loading in H-mode. With the $Re(Z_T) = 3.0\text{-}j2.5\Omega$ resilient loading condition, the $VSWR_{kl}$ (traces 3) remain below the 3.0 trip limit, also during ELMs. The $SMAD_{kl}$ error signals (traces 4) show the remaining noise level (15-20%) and a number of spurious (single) error points) for the $SMAD_{78}$, due to an (at that point in time, see Table 1) unresolved electronics problem. Figure 3 zooms in on the only generator power trip at 16.71s, where $SMAD_{78}$ (trace 4) Figure 3 (b) shows more than 10 consecutive error points clearly above the trip limit of 0.3 and this triggers the logical inverted NOT($SMAD_{78}$) trip signal (trace 5) to drop to arc = 0 (fail-safe, no arc = 1).

Note that the $VSWR_{kl}$ (traces 3) remain below the trip limit until the signal amplitudes fall

below their minimum acceptable value (~5kV for the probe voltages). The $SHAD_{kl}$ logical signals are not hard-wired to the trip system, are not fail-safe inverted (no arc=0) and do not confirm the SMAD detection in this case. The interpretation is that the ELM does not cause arcing directly on the straps, but inside the SMAD monitored region due to the changing voltage amplitude.

Figure 4 (a) illustrates **JET Pulse No. 78073** with $B_T = 2.7T$, $I_p = 1.9MA$, no neutral beam power $P_{NBI} = 0MW$. The ILA upper half E12+E56 is coupling $P_{ICRF} = 2.2MW$ into this L-mode plasma at $42MHz$ and $Re(Z_T) = 3\text{-}j0.5\Omega$. The D_α signal (trace 1) indicates no significant plasma ELM activity, with the strap voltages (trace 2) increasing gradually to ~40kV as the plasma separatrix is retracted gradually from 5.0-6.0cm from the first wall. The $VSWR_{56}$ (trace 3) is well below the trip limit 3.0, with several trip events occurring after 12s when the voltage reaches its maximum. The $SMAD_{56}$ error signal (trace 4) is at its normal noise level except during the trip events. The last trace (5) shows that the $SMAD_{56}$ system does not generate any of the trips, while the $SHAD_{56}$ signal gives indication of arcing on most trip events, but not all, depending on the level of arc activity and SHAD sensitivity settings. Figure 4 (b) zooms in on the first trip event 12.3-12.31s and shows the $SHAD_{56}$ indication of arcing (trace 5), combined with a gradual increase of the $VSWR_{56}$ (trace 3) and a low $SMAD_{56}$ error signal (trace 4) up to the point where the $VSWR_{56}$ protection shuts down the power. The interpretation is that arcing occurs outside the SMAD monitored region (see Figure 1), most likely on the straps, where the symmetrical decrease of voltages on the straps (trace 1) would indicate simultaneous arcing, or also possible is arcing on the common feed line.

Figure 5 (a) shows **JET Pulse No. 78052**, with $B_T = 2.7T$, $I_p = 1.7MA$, $P_{NBI} = 22MW$ from 4.0-8.0s, at first wall to separatrix distance $7.0cm$. The ILA upper half E12+E56 (only E12 shown) couples $P_{ICRF} = 1.5MW$ into an ELMy H-mode plasma at $42MHz$ and $Re(Z_T) = 3\text{-}j0.5\Omega$.

The D_α signal (trace 1) indicates significant ELM activity, with the strap voltages (trace 2) reaching $\sim 35kV$. Several generator trips occur throughout the pulse, with $VSWR_{12}$ (trace 3) and $SMAD_{12}$ (trace 4) generated trips, some of which confirmed by the $SHAD_{12}$ system (trace 5). Figure 5 (b) zooms in a sequence of events from 5.780-5.785s, where an ELM at 5.7825s (trace 1) generates an arc on strap 2 (asymmetrical voltages on trace 2), which is not detected by the SHAD system (trace 5), but generates an increase in the $VSWR_{12}$ (trace 3), still below the trip limit allowing the generator to continue applying power. The $SMAD_{12}$ error (trace 4) gives indication of an event starting to occur inside the SMAD monitored region, but not severe enough to trip the system until 5.784s. Figure 6 (b) zooms in further on this event, where clearly a significant time after the occurrence of the ELM (traces 1 on Figure 6 (a) and (b), a clear rise in the $SMAD_{12}$ error signal (trace 4) at 5.7838s and confirmed by the $SHAD_{12}$ system (not connected see Figure 1) starts the shutdown of the generator. This sequence of events is a good example of an arc on the strap causing a redistribution of the voltage/current patterns over the system that then causes an arc inside the SMAD monitored region and highlights the need for human interpretation of fast electrical arcing over a spatially extended system.

Figure 7 (a) and (b) show **JET Pulse No. 77743**, with $B_T = 2.15T$, $I_p = 1.95MA$, $P_{NBI} = 12MW$ from 14.0-17.0s, and first wall to separatrix distance kept at $5.0cm$. The ILA lower half E34+E78

is coupling $P_{ICRF} = 0.20MW$ at $33MHz$ and $Re(Z_T) = 3\text{-}j0.5\Omega$. This RF pulse is performed at low power and voltages 8-12kV to allow adjustment of the matching settings for E78. Note that the SMAD error signals (traces 4) show a higher noise level (of unknown origin) than on other the examples and this necessitated a higher SMAD trip limit setting 0.5. This RF pulse is of interest, since all consecutive RF pulses indicated a vacuum failure of capacitor C7, not able to sustain any RF voltage above the detection limit. The question than arises as to why the $SMAD_{78}$ error signal would not detect such a failure. A time zoom on the end of the pulse in Figure 8 (c) and (d) shows the SMAD error signal deteriorating as the amplitude of the probe voltages (traces 2) goes down, but no indication of arcing or vacuum failure by $SMAD_{78}$ or $VSWR_{78}$ down to $\sim 2kV$. It is likely that bellows puncture occurred after the end of the pulse, during the movements of the capacitor to their extreme parked position. However, investigating the possible occurrence of series arcs inside the vacuum capacitor with circuit simulation (modeled with varying values of a inductances [3]) revealed that such a fault condition would not generate a SMAD error signal higher than the usual trip level setting of (trace 4) ~0.2 in any case.

CONCLUSIONS

Despite the simplicity of the basic idea, the commissioning of the 4 SMAD systems on the JET-ITER-Like antenna was a protracted and technically challenging process. However, the system has become fully functional under a variety of RF (42 and $33MHz$, T-point impedances from $Re(Z_T) = 6\Omega$ to $Re(Z_T) = 3\Omega$, high and low voltage) and plasma loading conditions (L-mode, ELMy H-mode, different first wall-plasma separatrix distances) and has allowed the ILA to couple power into ELMy H-mode plasmas whilst being protected against arcing in the T-point low impedance zone. Examples of data analysis demonstrate the complicated nature of real electrical arcing events on a distributed system of 4 interacting strap pair resonators and feeding lines. Further investigation into the operation of the system has shown some shortcomings in the present implementation. The presently used Equation (1) detects arcs at the T-point, but is insensitive in other spatial regions [2], and the occurrence of series arcs in the vacuum capacitors (protected by the VSWR system on the ILA), which could be resolved by testing and combining several error equations. Further testing on the JET A2 antennas and transmission line arc test stands is being considered and might lead to future implementation in more general signal consistency check arc detection systems on the ITER ICRF launchers.

ACKNOWLEDGMENTS

This work, supported by the European Communities under the contract of Association between EURATOM and Belgian state and between EURATOM and UKAEA, was carried out within the framework of the European Fusion Development Agreement. The views and opinions expressed herein do not necessarily reflect those of the European Commission. The work carried out by UKAEA personnel was also funded by the United Kingdom Engineering and Physical Sciences Research Council.

REFERENCES

[1]. F. Durodié, Ph. Chappuis, J. Fanthome, R.H. Goulding, J. Hosea, P.U. Lamalle, A. Lorenz, M.P.S. Nightingale, L. Semeraro, F. Wesner, Main Design Features and Challenges of the ITER-Like ICRF Antenna for JET, Fusion Engineering and Design, **74** (2005), pp 223-228.

[2]. M. Vrancken, E. Lerche, T. Blackman, P. Dumortier, F. Durodié, M. Evrard, R.H. Goulding, M. Graham, S. Huygen, P. Jacquet, A. Kaye, M.-L. Mayoral, M.P.S. Nightingale, J. Ongena, D. Van Eester, M. Van Schoor, M. Vervier, R. Weynants, Operational Experience with the Scattering Matrix Arc Detection System on the JET ITER-Like Antenna, AIP Conference Proceedings 1187, (2009), pp. 237-240.

[3]. M. Vrancken, A. Argouarch, T. Blackman, P. Dumortier, F. Durodié, M. Evrard, R.H. Goulding, M. Graham, S. Huygen, P. Jacquet, A. Kaye, E. Lerche, M.P.S. Nightingale, D. Van Eester, M. Vervier, et al., Scattering Matrix Arc Detection on the JET ITER-Like ICRH Antenna, Fusion Engineering and Design D, **84**(2009), pp. 1953-1960.

[4]. P. Jacquet. G. Berger-By, V. Bobkov, T. Blackman, F. Durodié, M.-L. Mayoral, M.P.S. Nightingale, Characterisation of the Sub-Harmonic Arc Detection System on JET ITER-Like Antenna, AIP Conference Proceedings 1187, (2009), pp.241-244.

Pulse No:	Date	Description	Data collection
75196	08/10/2008	Automated data collection	# 570, 85GB compresses
76167	09/12/2008	SMAD on-line protection	# 400, 60GB
77453	05/03/2009	Last error correction	# 160, 25GB
78136	07/04/2009	End experiment 20009	

Table 1: Overview of commissioning SMAD system during JET experiments 2008-2009.

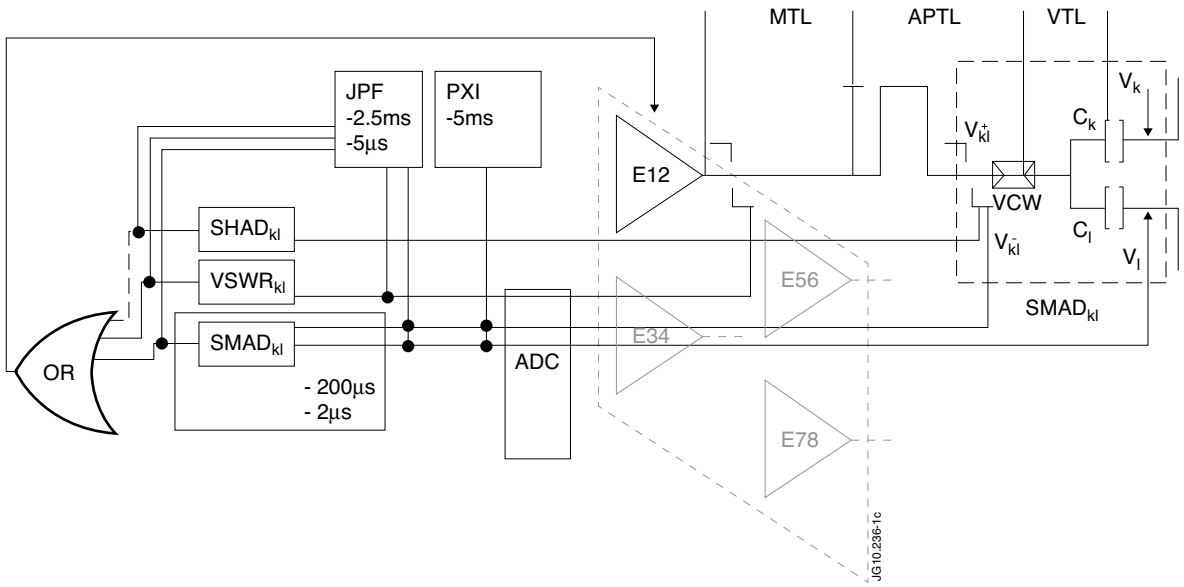

Figure 1: One quarter (strap pair 12) of ILA antenna with routing of the signals into VSWR, SHAD and SMAD arc detection systems and PXI, JPF and SMAD data storage systems. A similar signal routing applies for the other pairs kl. The resulting trip signal controls all 4 amplifiers together.

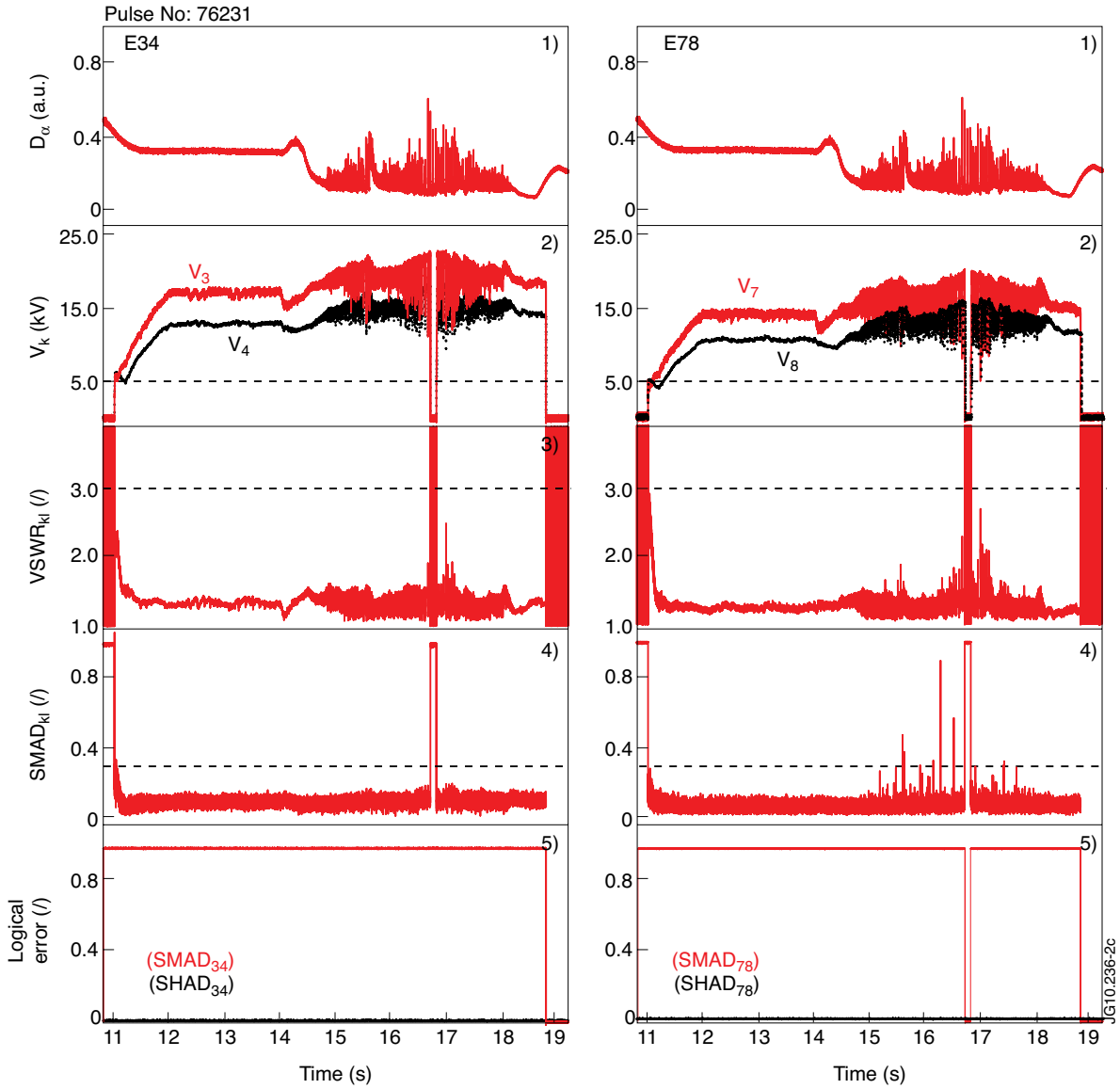

Figure 2: JET Pulse 76231 with ILA lower half E34+E78 coupling 0.4MW at 18 to 24kV strap voltage into L- and ELMy H-mode plasma. One generator trip occurs at 16.71s.

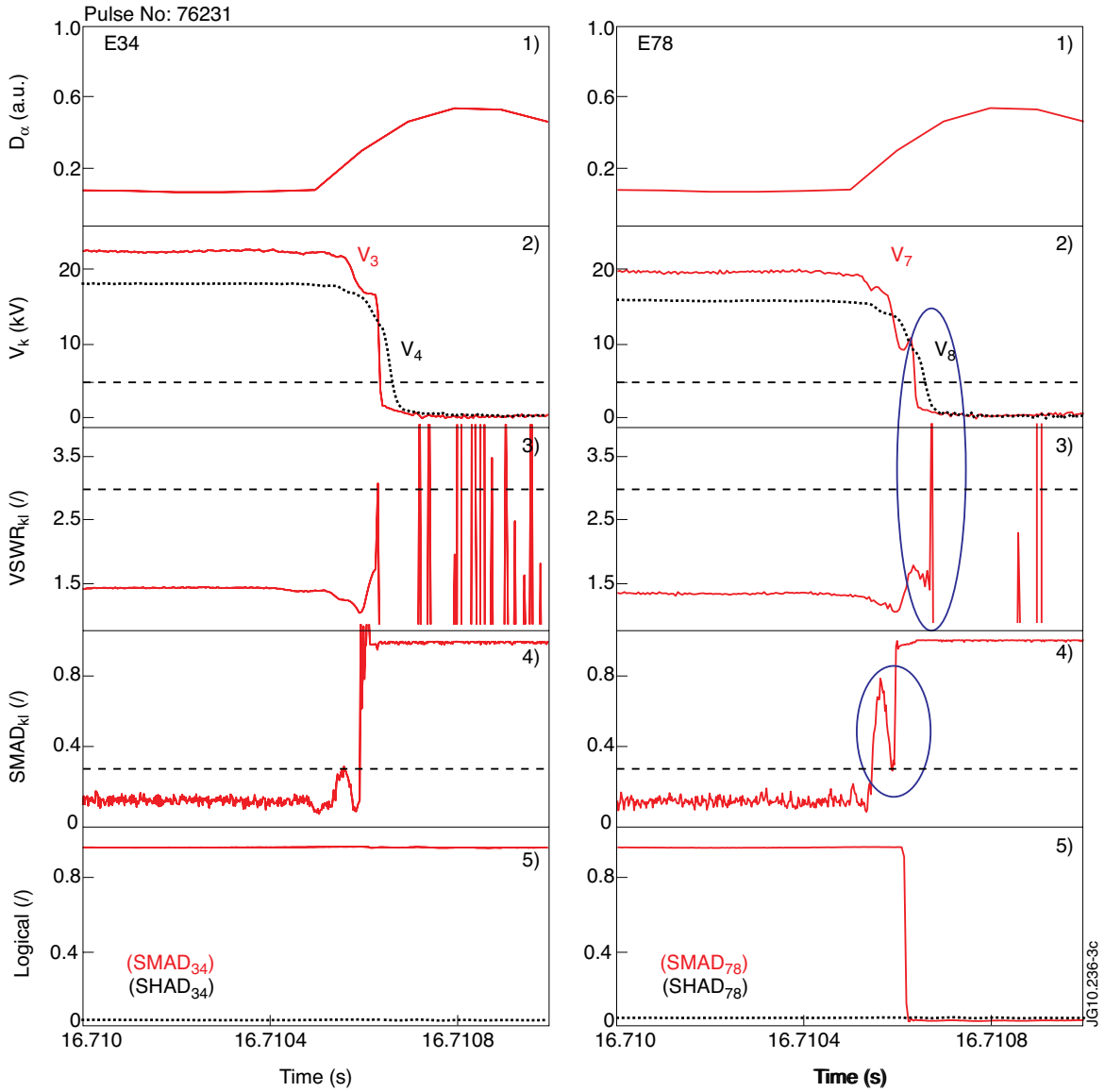

Figure 3: JET Pulse 76231 time zoom 16.710-16.711s on generator power trip, caused by a SMAD arc detection on E78.

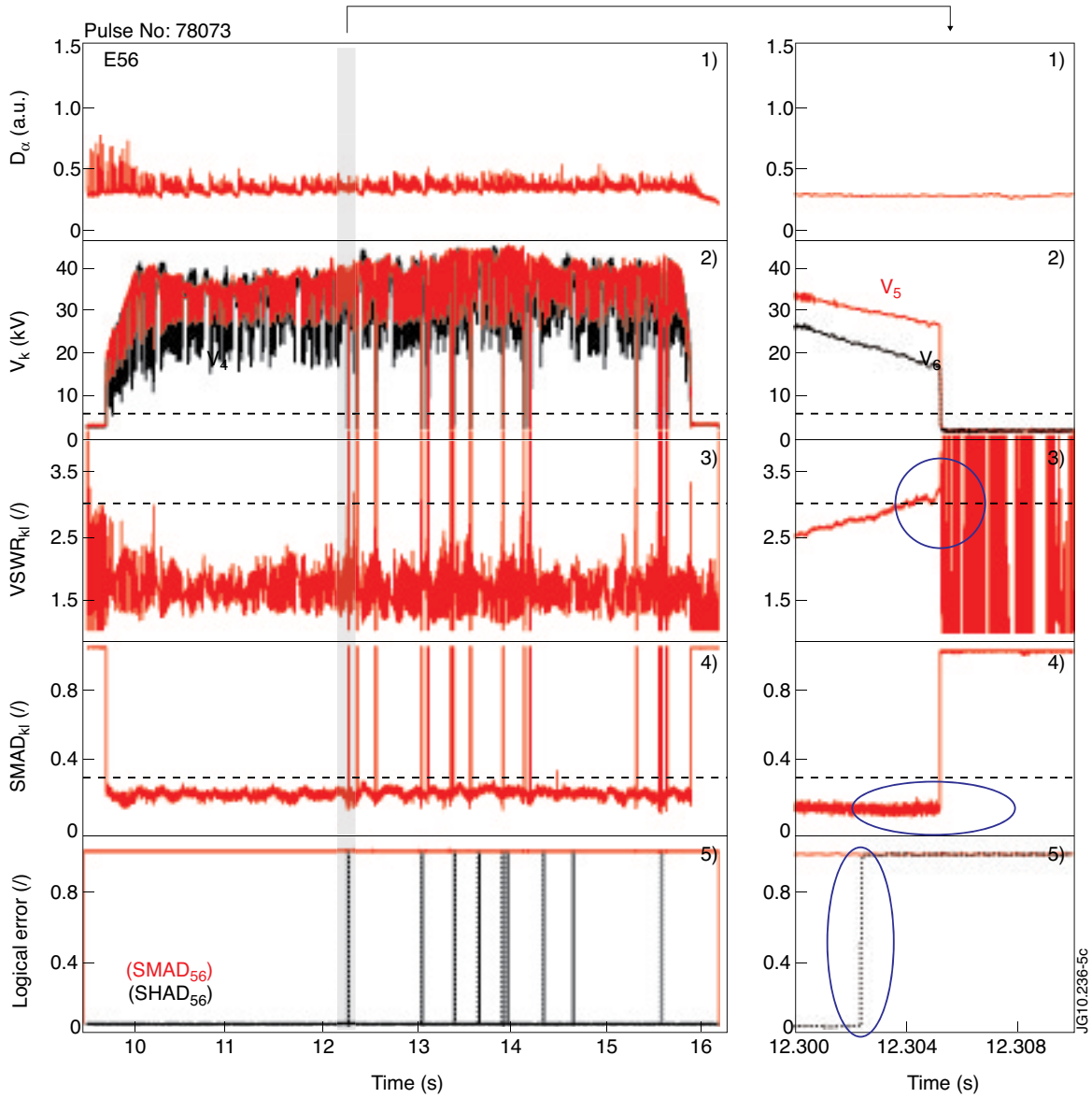

Figure 4: JET Pulse 78073 with ILA upper half E12+E56 (only E56 shown) coupling 2.2MW at 40kV strap voltage (a) 10.8-16.2s (b) Time Zoom 12.3-12.31s. A clean SMAD56 error signal combined with SHAD56 and increase in VSWR56 indicate arcing outside the SMAD monitored region.

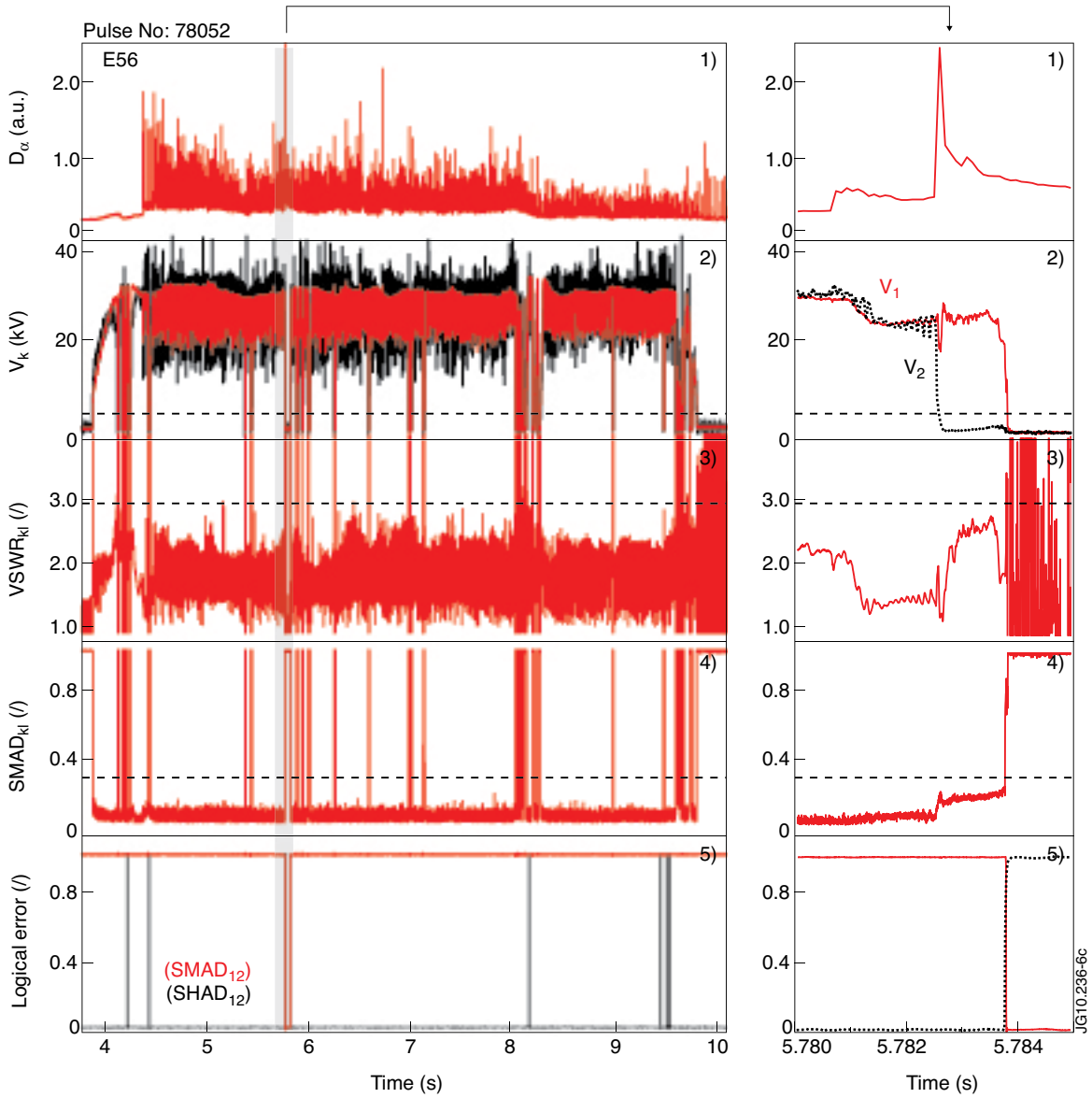

Figure 5: JET Pulse No. 78052 with ILA upper half E12+E56 (only E12 shown) coupling 1.5MW at 35kV strap voltage (a) 3.8-10.2s (b) Time Zoom 5.780-5.785s. An ELM at 5.7825s generates and arc on strap 2, but does not stop the generators until another event occurs at 5.784s.

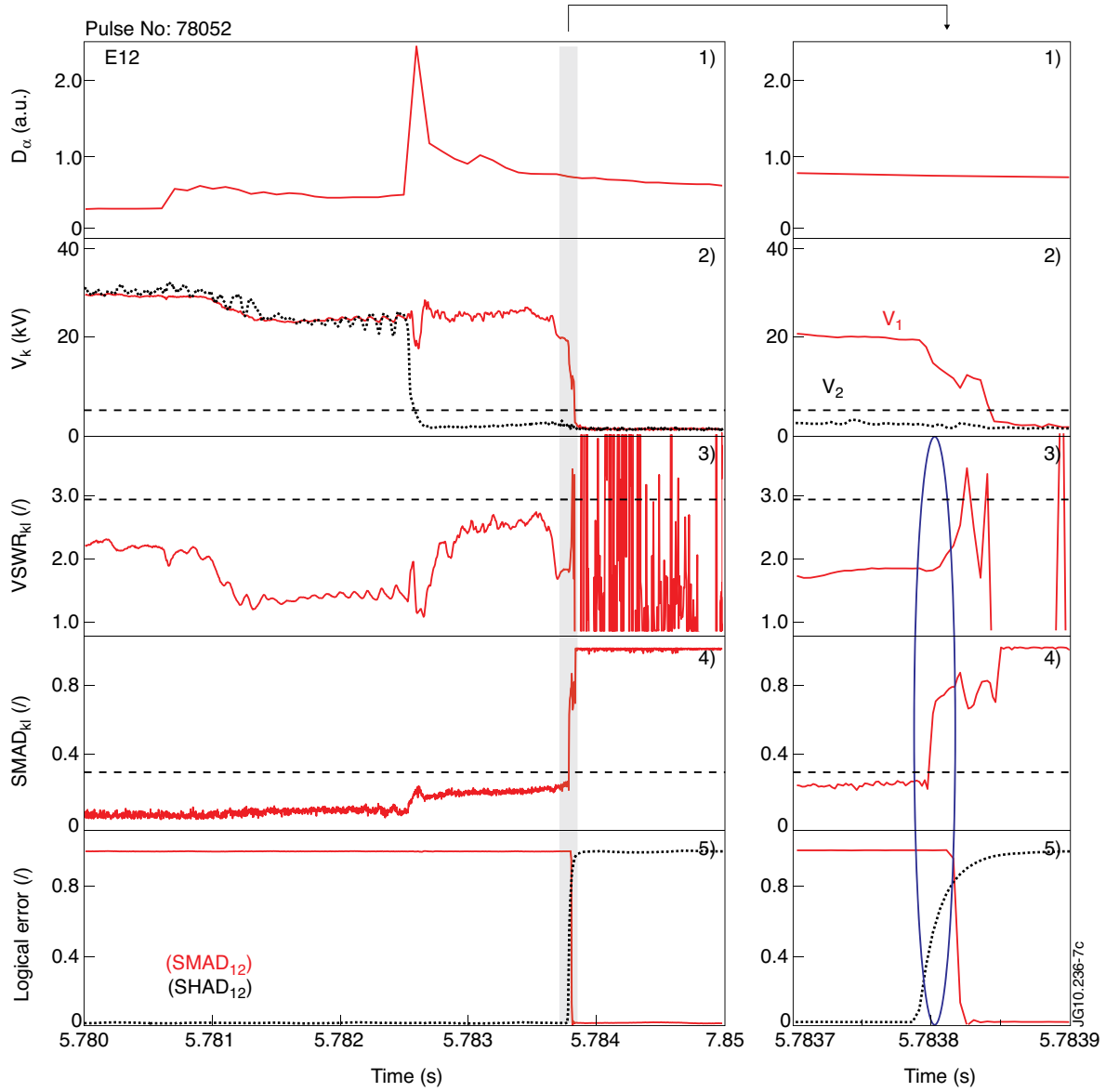

Figure 6: JET Pulse No. 78052 (a) 5.780-5.785-10.2s (b) further time zoom 5.7837-5.7839s. The ELM induced arc on strap 2 (trace 2 on (a) at 5.7825s) generates a second arc at 5.7838s inside the SMAD monitored region as confirmed by SMAD12 and SHAD12 traces 4 and 5 on (b).

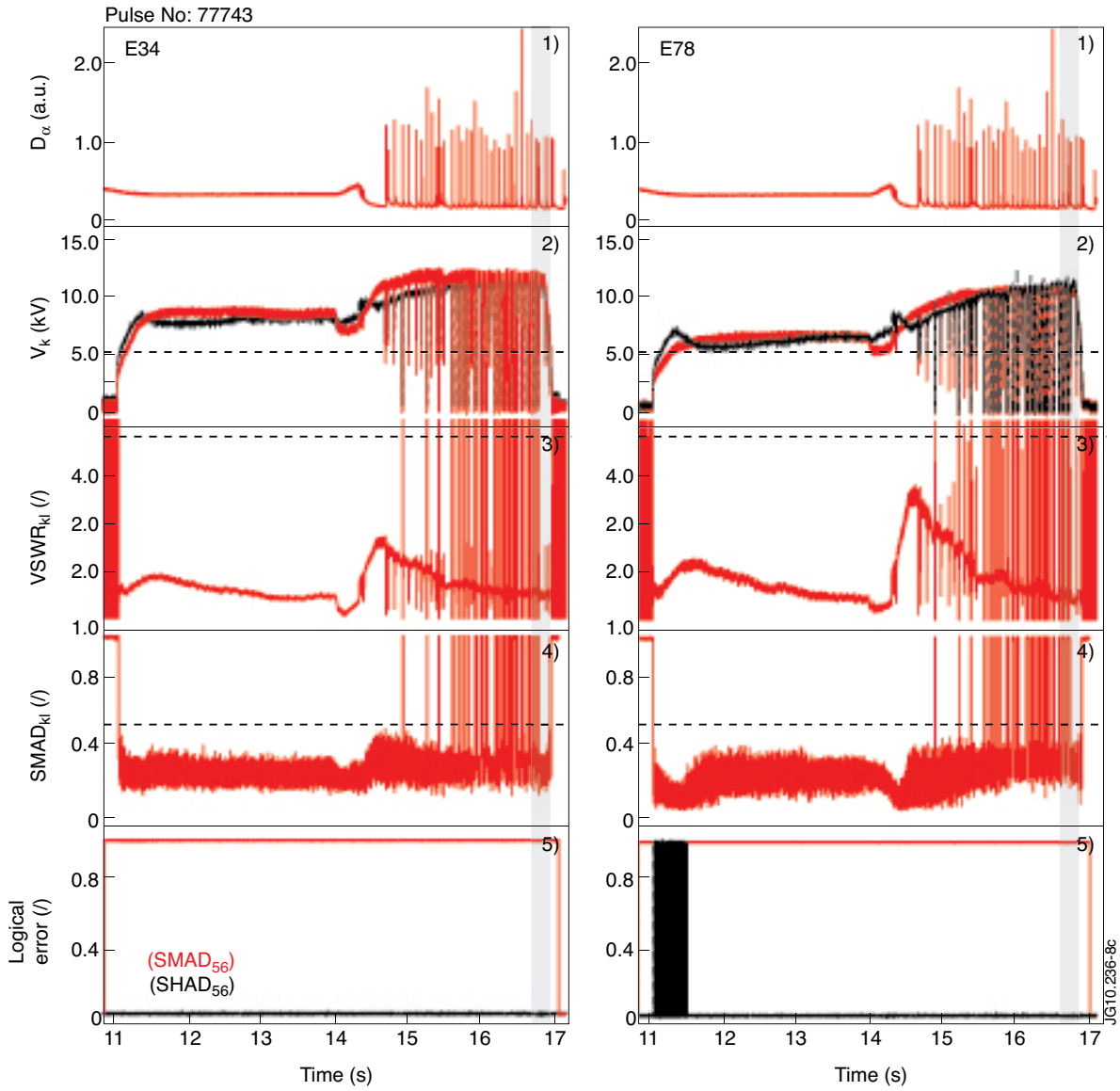

Figure 7: JET Pulse 77743 with ILA lower half E34+E78 coupling 0.2MW at 8 to 12kV strap voltage at 33MHz.

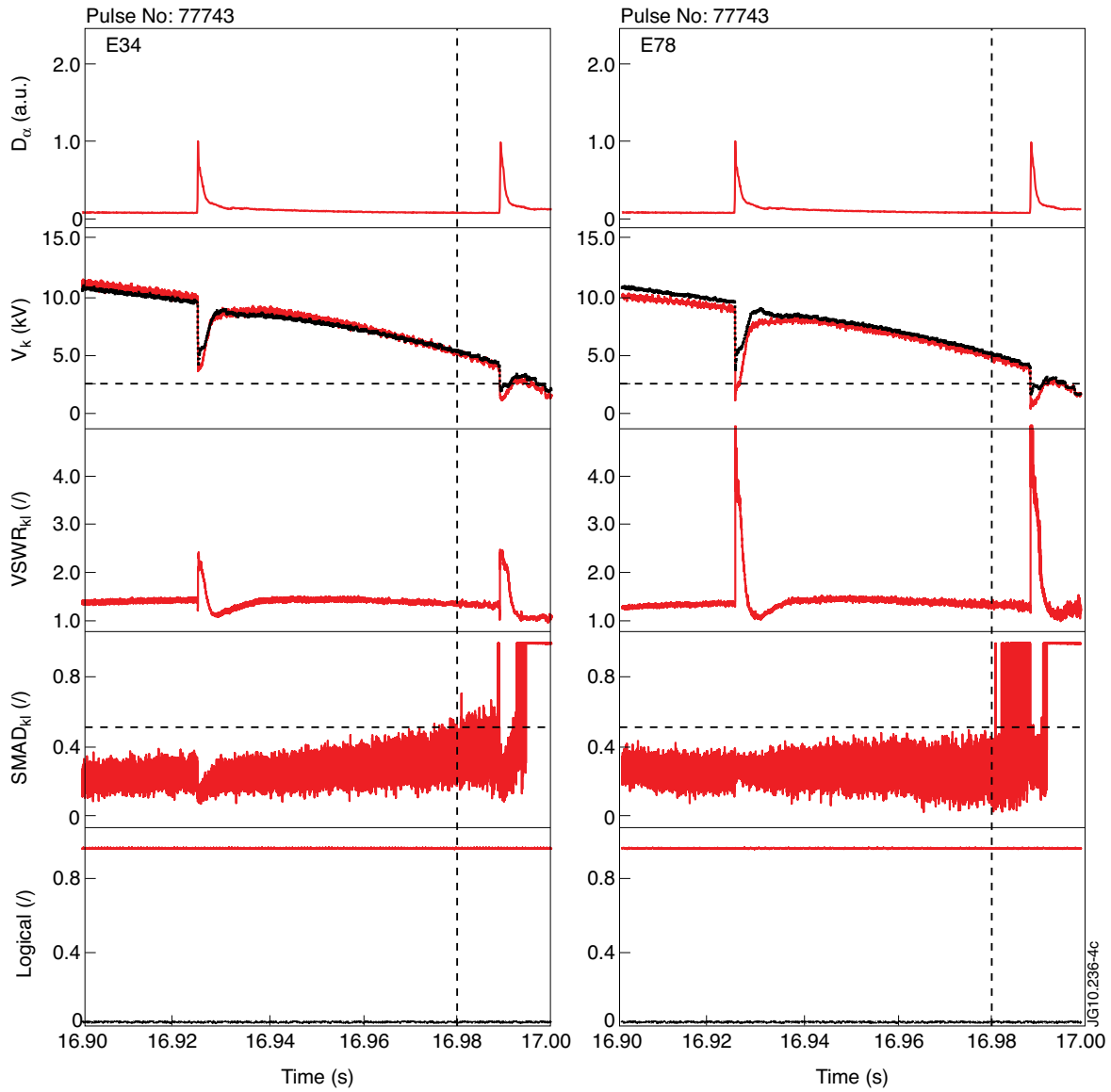

Figure 8: JET Pulse 77743 time zoom at the end of the pulse 16.9-17.0, showing normal behaviour during power shutdown and no indication of arcing or vacuum failure of capacitors.